

Arsenic-flux dependence of surface morphology in InAs homoepitaxy

Akihiro Ohtake ^{1,a)}, Takuya Kawazu ¹ and Takaaki Mano ¹

¹National Institute for Materials Science (NIMS), 1-1 Namiki Tsukuba, Ibaraki 305-0044

a) Electronic mail: OHTAKE.Akihiro@nims.go.jp

Abstract

Surface morphology in molecular-beam epitaxy of InAs(001), (111)A, and (111)B has been studied using scanning tunneling microscopy. The surface morphologies of InAs strongly depend on the substrate temperature, the substrate orientation, and the As/In flux ratio. The size and density of two-dimensional InAs islands on the (001) surface decreases and increases, respectively, as the As/In flux ratio is increased. On the other hand, the island size (density) is increased (decreased) with increasing the As flux on the (111)A and (111)B surface. Surface reconstructions on the growing surface strongly affect the diffusion and incorporation kinetics of In atoms, resulting in the observed surface morphologies.

I. INTRODUCTION

Molecular-beam epitaxy (MBE) has enabled the fabrication of heterostructures of a wide variety of materials, especially III-V semiconductors. The electrical and optical properties of the heterostructures critically depend on the interface morphology. Thus, deeper understanding of the mechanism controlling surface morphology is of primary importance. Since the MBE growth proceeds far from equilibrium, various parameters such as the growth rate, the substrate temperature, and the V/III flux ratio affect the surface morphology of the MBE-grown III-V surfaces. Among these parameters, the effect of the V/III flux ratio on the surface morphology is still controversial. It has been widely accepted that the migration of Ga atoms is enhanced in GaAs homoepitaxy under As-deficient conditions, resulting in the improved surface morphology and crystalline quality.¹ On the other hand, the contradictory results have been reported: the migration of Ga (In) on GaAs (InAs) is enhanced as the As flux is increased.²⁻⁵ Thus, the simple question still remains unanswered as to whether higher or lower V/III ratio is favorable in improving surface morphology.

This paper reports a systematic study on the surface morphology of epitaxially growing InAs on the (001)-, (111)A, and (111)B-oriented substrates. InAs homoepitaxy was chosen as it avoids the complications associated with lattice mismatch and intermixing. Using scanning tunneling microscopy (STM), we show that the surface morphology strongly depends on the substrate temperature, the substrate orientation and the V/III flux ratio. The density of two-dimensional InAs islands on the (001) surface increases with increasing V/III ratio, while the densities for the (111)A and (111)B

surfaces are decreased. We found that surface reconstructions play a key role in determining the observed arsenic-flux dependence of surface morphologies.

II. EXPERIMENTAL

The growth experiments were carried out in a multi-chamber MBE system.^{7,8} Non-doped and nominally on-axis InAs(001), InAs(111)B, and InAs(111)A substrates were used for the growth experiments. The clean surfaces were prepared by growing undoped homoepitaxial layers (10 nm thick) at 450°C on thermally cleaned InAs substrates. After being annealed at 550°C for 1 hour under the As₂ flux of 5.7x10⁻⁵ Pa, the substrates were cooled to 400-500°C under the As₂ flux. The (001) surface shows (2x4) and (4x2) reconstructions, and the (111)B surface shows (1x1) and (2x2) reconstructions, depending on the substrate temperature, while only a (2x2) reconstruction is observed on the (111)A surface.

The 4ML-thick InAs films were grown using a conventional Knudsen cell for In and a valved cracker cell for As₂. The beam-equivalent pressures (BEPs) of In and As₂ were measured using a beam flux monitor at the sample position. The BEP of In was controlled at 8.6 x10⁻⁷ Pa and that for As₂ was varied in the range of 6.8 x10⁻⁶ to 8.2 x10⁻⁵ Pa (BEP ratio ranging from 8 to 95). The growth process of InAs was monitored by reflection high-energy electron diffraction (RHEED) in real time with an electron-beam energy of 15 keV. The growth rate of InAs was approximately 0.027 ML/s, which was calibrated by RHEED intensity oscillation measurements on the (001)-oriented InAs substrate. Here, 1 ML of InAs is defined as 6.3x10¹⁴ atoms/cm², which is the site-number density of unreconstructed InAs{111} surface.

To quench the surface morphology as it appeared during the growth, the samples were rapidly cooled immediately after the In and As molecular beams were simultaneously turned off, and were subsequently rotated by 180° away from the direction of In and As₂ molecular beams. The samples were then transferred via UHV transfer modules to another UHV chamber for the STM observations. All the STM images were collected at room temperature in the constant current mode with a tunneling current of 0.1 nA and a sample voltage of -3 V.

III. RESULTS AND DISCUSSION

A. *InAs(001)*

Figure 1 shows a series of STM images taken after the growth of 4 ML-InAs on the InAs(001) surface at 400, 450, and 500°C. The surface morphology strongly depends on both substrate temperature and the As/In BEP ratio. The InAs film grown at 400°C shows a high density of islands and holes with 1 ML-height. The density of InAs islands decreases with increasing substrate temperature, indicating that the migration of In atoms is thermally activated at high temperatures, so that the direct incorporation of adatoms at the existing step edges is enhanced.

The growing surfaces show (2x4) and (4x2) reconstructions depending on the substrate temperature and the As/In BEP ratio: typical magnified STM images are shown in Fig. S1 in Supplementary Material. The surface shows the As-rich (2x4) reconstruction under higher BEP ratios and/or at lower substrate temperatures, while the In-rich (4x2) reconstruction appears as the BEP ratio and the substrate temperature decreases and increases, respectively. The islands on the As-rich (2x4) surface are

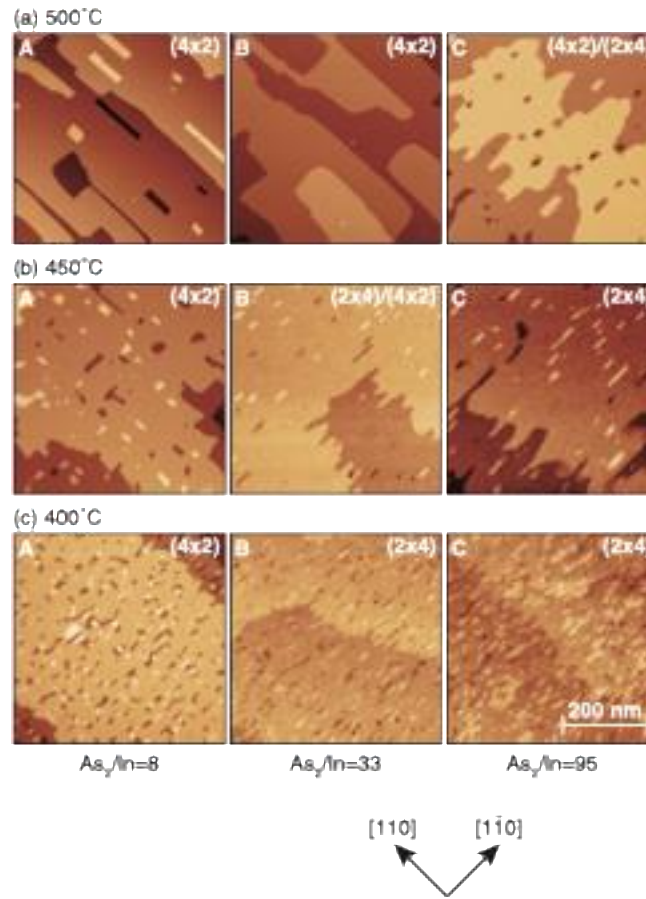


Figure 1: STM images of 4ML-InAs grown on InAs(001) at 500°C (a), 450°C (b), and 400°C (c). The image dimensions are 500 nm x 500 nm. The as-grown films show (2x4), (4x2), and mixed (2x4)/(4x2) surface structures depending on the As flux and substrate temperature, as indicated in the images.

extended in the $[1-10]$ direction, while those on the In-rich (4x2) surface are slightly elongated along the orthogonal direction of $[110]$. The surface atomic structures of the (2x4) and (4x2) surfaces have been well established: β_2 structure [Fig. 2(a)] for (2x4)^{9,10} and the ζ structure [Fig. 2(b)] for (4x2)^{11,12} are commonly formed on InAs(001) and GaAs(001) surfaces. Previous studies have shown that the activation energy of the diffusion of Ga atoms on the GaAs(001) surface is highly anisotropic: the diffusion

barrier along the $[1-10]$ direction is significantly smaller than that in the $[110]$ direction on the $\beta 2(2 \times 4)$ surface,¹³ while the diffusion along the $[110]$ direction is favored on the $\zeta(4 \times 2)$ surface.⁷ It is suggested, therefore, that the anisotropic surface morphology stems from the anisotropic surface diffusion of In atoms. In addition, we note that the one-dimensional islands extending along the $[1-10]$ direction on the (2×4) surface is more stable than that elongated along the $[110]$ direction: according to the electron counting model,¹⁴ the former structure [Fig. S2(a)] in Supplementary Material) has no partially-filled dangling bonds. Similarly, the island structures on the (4×2) surface extending along the $[110]$ direction [Fig. S2(b)] also satisfy the electron counting rule.

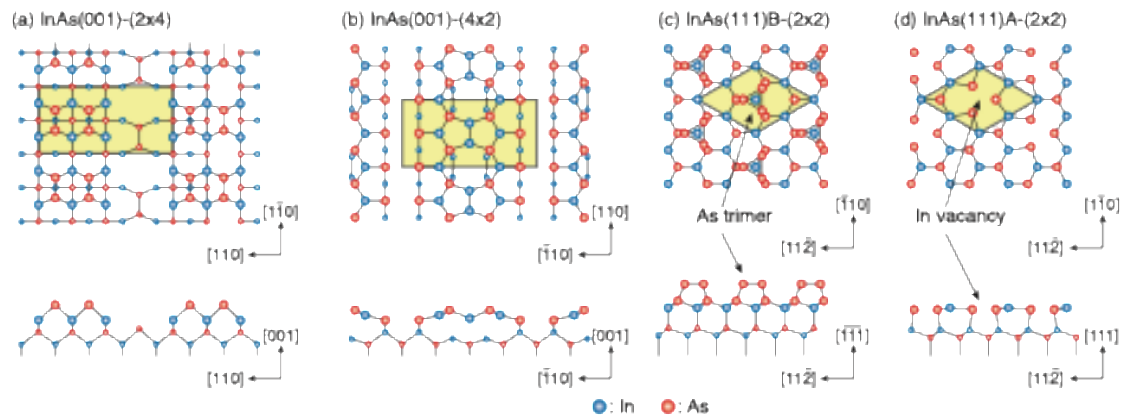


Figure 2: Structure models for InAs(001)-(2x4) (a), InAs(001)-(4x2) (b), InAs(111)B-(2x2) (c), and InAs(111)A-(2x2) (d) surfaces.

To characterize the surface morphologies, total lengths of edges of steps and islands have been estimated; the edge length has been proved to be an adequate characteristic of surface morphology.¹⁵ The results are shown in Fig. 3(a), in which the length of edges in STM images (500 nm x 500 nm) are plotted as a function of the As/In BEP ratio. For the InAs films grown at temperatures of 450 and 500°C, the edge lengths are significantly shorter than those on the sample grown at 400°C, and do not strongly

depend on the BEP ratio. At a lower temperature of 400°C, on the other hand, the edge length increases with increasing BEP ratio. This means that the increased As flux disturbs the diffusion of In atoms at 400°C, so that In atoms react with arriving As molecules to form InAs nuclei on terrace, before being incorporated at edges of steps/islands.

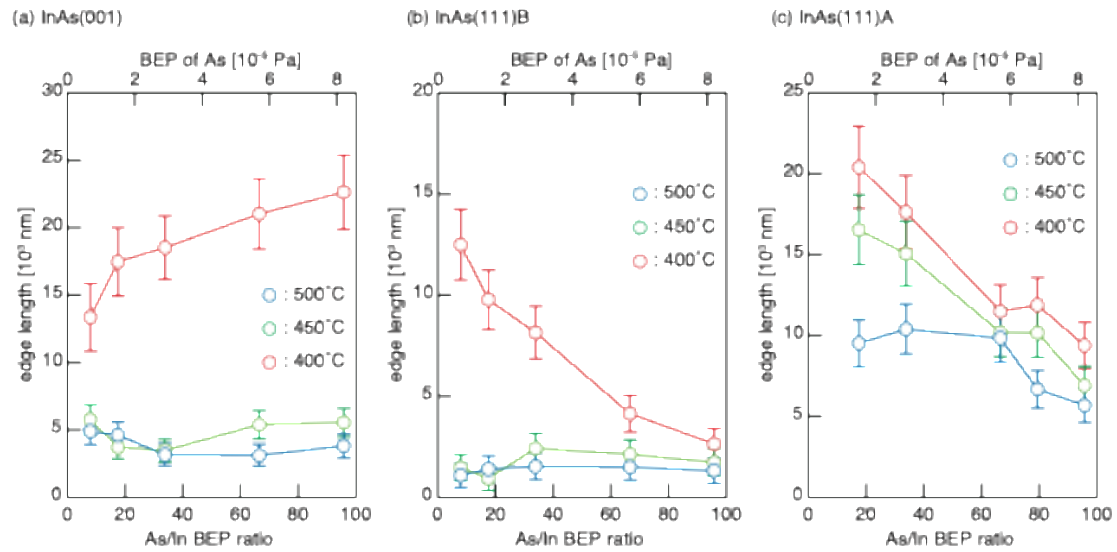


Figure 3: Total lengths of step and island edges estimated from the STM images (500 nm x 500 nm) for InAs(001) (a), InAs(111)B (b), and InAs(111)A (c) plotted as a function of the As/In BEP ratio.

Here, it is interesting to note that the edge length drastically decreases as the BEP ratio is decreased from 17 to 8 at 400°C. The results could be explained as follows. The initial InAs surface shows a (2x4) reconstruction in the whole range of the As BEP at 400°C. The (2x4) reconstruction was preserved throughout the growth with the BEP ratios ranging from 17 to 95. On the other hand, when the InAs films were grown with the BEP ratio of 8, the surface structure gradually changed from (2x4) to (4x2), indicating that the (2x4) and (4x2) reconstruction coexist during the 4 ML-growth. As mentioned

earlier, the migration on the (2x4) and (4x2) surfaces show a strong anisotropy: longer diffusion lengths in the [1-10] and [110] directions for (2x4) and (4x2), respectively. Thus, it is likely that the coexistence of (2x4) and (4x2) reconstructions facilitates more isotropic diffusion of In atoms, and effectively increases the diffusion area, resulting in the decrease in the nucleation probability on the terrace. This is consistent with the less anisotropic shape of InAs islands grown with the BEP ratio of 8 at 400°C [Fig. 1(c)-A].

The present results are in good agreement with those reported by Bell et al. for GaAs(001),¹⁶ which have been supported by kinetic Monte-Carlo simulations.¹⁷ This is compatible with the common belief that the surface diffusion is enhanced when the As flux is reduced: the extreme case is the alternating supply of In (Ga) and As fluxes, which is called migration enhanced epitaxy.¹ On the other hand, contradictory experimental and theoretical results have been reported for InAs(001)²⁻⁴ and GaAs(001);^{5,6} the growth with the higher V/III ratio results in the fewer and larger two-dimensional islands. While the origin for such a discrepancy is unknown at the present stage, we point out that the growth rates employed in ref. 16 and this study are much lower than those in refs. 2-6, which might result in different surface morphologies.

B. InAs(111)B

Figure 4 shows STM images taken after the 4ML-growth on InAs(111)B. While two-dimensional islands are formed at a lower temperature of 400°C, the density of such islands is significantly decreased at higher temperatures above 450°C. The majority of islands have an equilateral-triangle shape. The edges of steps and triangle islands are perpendicular to the [-1-12] direction and equivalent [-12-1] and [2-1-1] directions. As

This is the author's peer reviewed, accepted manuscript. However, the online version of record will be different from this version once it has been copyedited and typeset.
PLEASE CITE THIS ARTICLE AS DOI: 10.1116/6.0003957

schematically shown in Fig. S3 in the Supplementary Material, there exist two types of atomic configurations of the step edges on the (111)B surface; one is $[-1-12]$, $[-12-1]$ and $[2-1-1]$, and the other is $[11-2]$, $[1-21]$, and $[-211]$. The former has only one dangling bond per edge In atom, whereas the latter has two dangling bonds per atom. Thus, the observed anisotropic morphology could be explained by the relative stability of steps. We note that some islands are rotated by 180° , which could be ascribed to the formation of rotational twin domains.

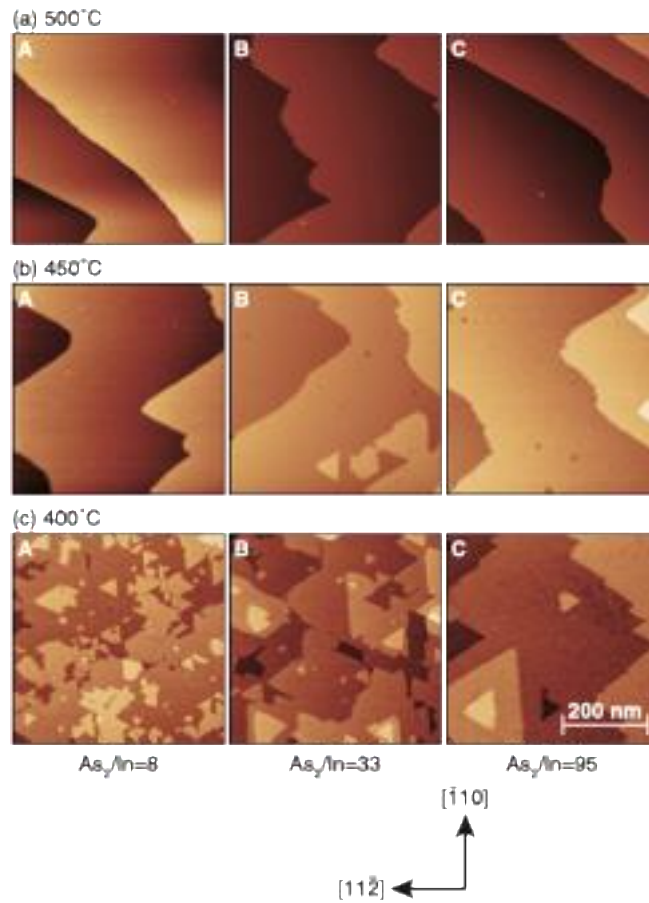


Figure 4: STM images of 4ML-InAs grown on InAs(111)B at 500°C (a), 450°C (b), and 400°C (c). The image dimensions are 500 nm x 500 nm.

Shown in Fig. 3(b) is the total length of step and island edges on InAs(111)B. The size and density of InAs islands on the (111)B surface are larger and lower than those on the (001) surface, indicating that the incorporation of In at the steps and existing islands is more favored than the formation of new InAs islands on the (111)B terrace. Similarly to the case for the (001) growth, the edge length hardly depends on the BEP ratio at 450 and 500°C. On the other hand, at a lower temperature of 400°C, in marked contrast with the (001) growth, the step length decreases with increasing BEP ratio.

The present results could be explained in terms of the atomic structure of the (111)B surface. As shown in Fig. 5(a), the magnified STM image taken from the 4ML-film grown with the BEP ratio of 33 shows bright protrusions spaced by ~2 nm, which is quite similar to that observed for the GaAs(111)B-($\sqrt{19}\times\sqrt{19}$)-R23.4° reconstruction.^{8,18} While the majority of bright protrusions are randomly distributed, ($\sqrt{19}\times\sqrt{19}$)-R23.4° units are locally observed, as shown in the inset of Fig. 5(a). Thus, it appears likely that the InAs(111)B surface under In-rich conditions has a disordered ($\sqrt{19}\times\sqrt{19}$) structure. The density of bright protrusions in the disordered ($\sqrt{19}\times\sqrt{19}$) structure decreases with increasing BEP ratio, as shown in Figs. 5(b) and 5(c), and the (2x2) reconstructions are clearly visible on the film grown with the BEP ratio of 95. The (2x2) reconstruction has been commonly observed on the (111)B surfaces of GaAs and InAs prepared under the most As-rich condition.^{19,20} The widely accepted model for the (2x2) reconstruction consists of As trimers located on the outermost As layer [Fig. 2(c)].²¹⁻²³ For the successive growth on the (111)B-(2x2) surface with alternate stacking of In and As layers, the exchange reaction is required between arriving In adatoms and As atoms in the

trimer, preventing In atoms from being incorporated in to the lattice sites on the terrace, as pointed out by Hayakawa et al. for the GaAs growth.²⁴

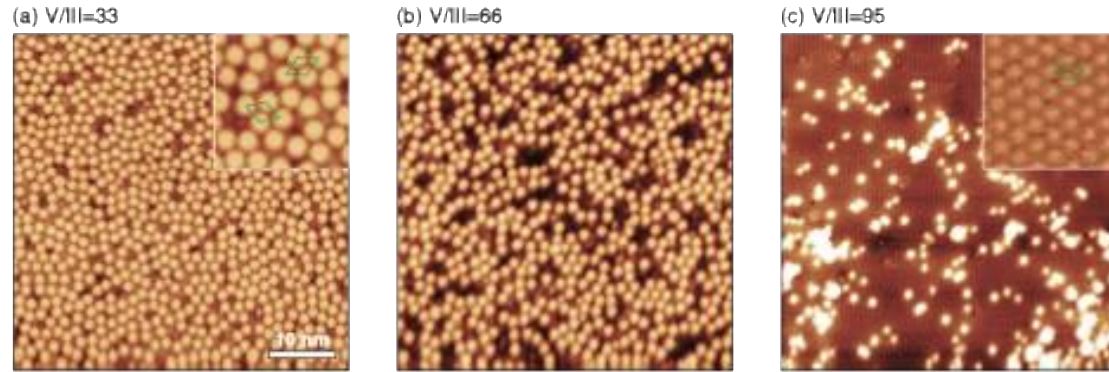


Fig. 5: Magnified STM images of the InAs(111)B films grown with the V/III BEP ratios of 33 (a), 66 (b), and 95 (c) at 400°C. The image dimensions are 50 nm x 50 nm. The inset in (a) and (c) show magnified images with dimensions of 10 nm x 10 nm and 5 nm x 5 nm, respectively, in which ($\sqrt{19} \times \sqrt{19}$)-R23.4° (a) and (2x2) (c)

The increase of the As flux also affects the incorporation kinetics at the step edges; since the steps on the (111)B surface are terminated by In atoms (see Figure S2 in the Supplementary Material), the incorporation of In at the edges of steps and island requires the simultaneous supply of As atoms/molecules. This means that the In atoms are more effectively incorporated at the step/island edges under more As rich conditions, resulting in the decrease in the island density on the terrace and the increase in the island size.

C. InAs(111)A

Figure 6 shows STM images of InAs(111)A. Two-dimensional islands are observed in the whole ranges of substrate temperatures and BEP ratios. As shown in Fig. 3(c), the edge length decreases with increasing BEP ratio, as in the case for the (111)B

orientation. The size and density of islands are smaller and larger, respectively, than those on the (111)B surface, and the islands have an irregular shape. Thus, at first sight, it is suggested that the diffusion of In is less enhanced on the (111)A surface, as compared with the (111)B surface. On the other hand, previous density-functional theory (DFT) calculations have shown that the diffusion barrier of Ga adatoms on the GaAs(111)A surface is 0.4 eV,²⁵ which are significantly smaller than the values for the (001) and (111)B orientations:²⁶ a longest diffusion length is expected on the (111)A surface among the three surface orientations. Thus, it is suggested that the surface morphology is governed by the incorporation kinetics of In at the lattice sites on the (111)A surface.

As we will show below, the incorporation kinetics is closely related with the surface reconstruction of the (111)A surface. The InAs(111)A films show a (2x2) reconstruction irrespective of the growth conditions. It has been well established that the (2x2) surface of InAs(111)A²⁷ and GaAs(111)A^{23,28} has the vacancy buckling structure [Fig. 2(d)], in which 0.25ML of In/Ga is missing at the outermost layer. Thus, the successive growth of InAs(111)A with zincblende structure requires the In-vacancy site to be occupied by the In atom. On the other hand, DFT calculations have shown that the Ga-vacancy site is not the most energetically stable for the Ga adatom on GaAs(111)A,²⁵ and have predicted that the occupation of the vacancy site becomes energetically favorable when additional three As atoms are adsorbed and coupled with one Ga atom.²⁹

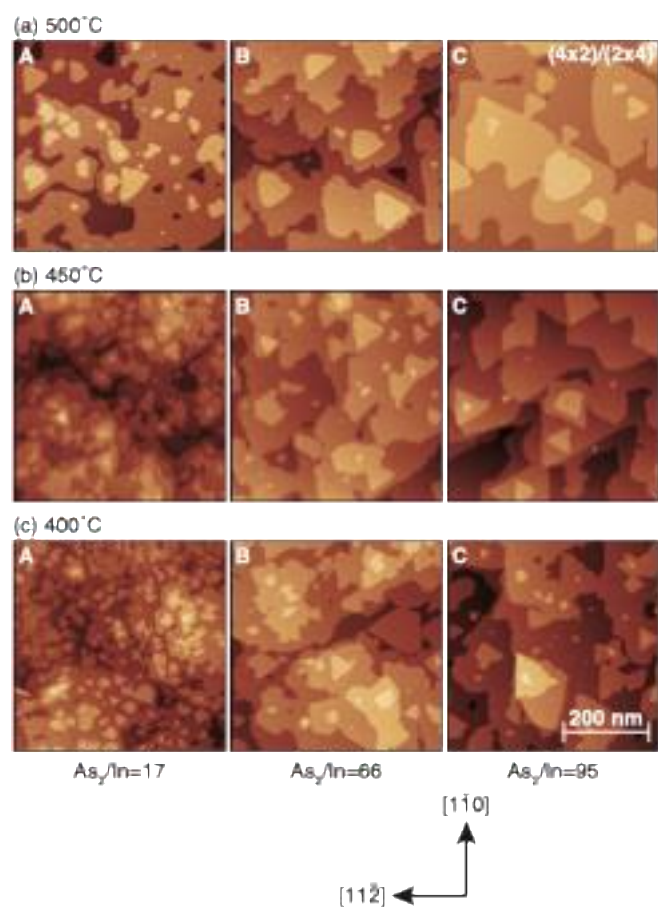


Figure 6: STM images of 4ML-InAs grown on InAs(111)A at 500°C (a), 450°C (b), and 400°C (c). The image dimensions are 500 nm x 500 nm.

Since the sticking probability of As₂ molecules on the (111)A surface is extremely low, it is suggested that the InAs growth occurs with the vacancy site being occupied by In only under As-rich conditions. Under As-deficient conditions, on the other hand, it is likely that In atoms form small droplets, leaving the vacancy site empty, and are not preferentially incorporated into the edges of islands/steps, similarly to the case for Ga on GaAs.⁸ Once small In droplets are formed on the (111)A terrace, they easily react with As molecules to form small InAs islands even under low As fluxes. Thus the decrease in the As BEP promotes the nucleation of small InAs islands on the (111)A terrace, but not the successive growth at edges of steps/islands. These explanations are in a good

agreement with the experimental results that the MBE growth of GaAs and InAs(111)A requires extremely high As fluxes.^{30,31}

IV. CONCLUSIONS

We have systematically studied the InAs homoepitaxy on the (001), (111)B, and (111)A-oriented substrates. The surface morphology of InAs strongly depends on the substrate orientation and the As/In BEP ratio. As the BEP ratio is increased, the densities of two-dimensional InAs islands are increased on the (001) surface, while those on the (111)A and (111)B surfaces are decreased. We found that surface reconstructions on the growing surfaces have significant effects on the diffusion and incorporation kinetics of In atoms, which well accounts for the observed As-flux dependence. While the present study focuses on InAs homoepitaxy, it is expected that the present finding also hold for GaAs, because InAs and GaAs show common surface reconstructions. The present results show that the precise control of the V/III BEP ratio is essential in obtaining flat surface in MBE growth of III-V semiconductors, especially at lower temperatures.

SUPPLEMENTARY MATERIAL

Magnified STM images of InAs(001); structure models for one-dimensional islands on InAs(001); schematic drawing of two-dimensional island on InAs(111)B.

ACKNOWLEDGMENTS

This work was partially supported by JSPS KAKENHI Grant Number JP23K04592.
Helpful discussions with J. Nakamura are gratefully acknowledged.

AUTHOR DECLARATIONS

Conflicts of Interest (*required*)

The authors have no conflicts to disclose.

DATA AVAILABILITY

The data that support the findings of this study are available from the corresponding author upon reasonable request.

REFERENCES

- ¹Y. Horikoshi, M. Kawashima, and H. Yamaguchi, Jpn. J. Appl. Phys. **25**, L868 (1986).
- ²F. Grosse, W. Barvosa-Carter, J. Zinck, M. Wheeler, and M.F. Gyure, Phys. Rev. Lett. **89**, 116102 (2002).
- ³J.H.G. Owen, W. Barvosa-Carter, and J.J. Zinck, Appl. Phys. Lett. **76**, 3070 (2000).
- ⁴H. Toyoshima, T. Shitara, P.N. Fawcett, J. Zhang, J.H. Neave, and B.A. Joyce, J. Appl. Phys. **73**, 2333 (1993).
- ⁵V.P. LaBella, D.W. Bullock, Z. Ding, C. Emery, W.G. Harter, and P.M. Thibado, J. Vac. Sci. Technol. A **18**, 1526 (2000).
- ⁶H. Yang, V.P. LaBella, D.W. Bullock, and P.M. Thibado, J. Vac. Sci. Technol. B **17**, 1778 (1999).
- ⁷A. Ohtake, T. Mano, A. Hagiwara, and J. Nakamura, Cryst. Growth Des. **14**, 3110 (2014).

- ⁸A. Ohtake, N. Ha, and T. Mano, *Cryst. Growth Des.* **15**, 485 (2014).
- ⁹C. Ratsch, W. Barvosa-Carter, F. Grosse, J.H.G. Owen, and J.J. Zinck, *Phys. Rev. B* **62**, R7719 (2000).
- ¹⁰T. Hashizume, Q.K. Xue, J. Zhou, A. Ichimiya, and T. Sakurai, *Phys. Rev. Lett.* **73**, 2208 (1994).
- ¹¹S.H. Lee, W. Moritz, M. Scheffler, *Phys. Rev. Lett.* **85**, 3890 (2000).
- ¹²C. Kumpf, L.D. Marks, D. Ellis, D. Smilgies, E. Landemark, M. Nielsen, R. Feidenhans'l, J. Zegenhagen, O. Bunk, J.H. Zeysing, Y. Su, R.L. Johnson, *Phys. Rev. Lett.* **86**, 3586 (2001).
- ¹³A. Kley, P. Ruggerone, and M. Scheffler, *Phys. Rev. Lett.* **79**, 5278 (1997).
- ¹⁴M.D. Pashley, *Phys. Rev. B* **40**, 10481 (1989).
- ¹⁵V.L. Alperovich, I.O Akhundov, N.S. Rudaya, D.V. Sheglov, E.E. Rodyakina, A.V. Latyshev, and A.S. Terekhov, *Appl. Phys. Lett.* **84**, 101908 (2009).
- ¹⁶G.R. Bell, M. Itoh, T.S. Jones, and B.A. Joyce, *Surf. Sci.* **423**, L280 (1999).
- ¹⁷O.A. Ageev, M.S. Solodovnik, S.V. Balakirev, and M.M. Eremenko, *J. Vac. Sci. Technol B* **34**, 041804 (2016).
- ¹⁸A.R. Avery, E.S. Tok, and T.S. Jones, *Surf. Sci.* **376** L397 (1997).
- ¹⁹D.A. Woolf, D.I. Westwood, R.H. Williams, *Appl. Phys. Lett.* **62**, 1370 (1993).
- ²⁰K. Sugiyama, *J. Cryst. Growth* **75**, 435 (1986).
- ²¹C.B.M. Andersson, U.O. Karlsson, M.C. Håkansson, L.Ö. Olsson, L. Ilver, P.-O. Nilsson, J. Kanski, P.E.S. Persson, *Phys. Rev. B*, **54** 1833 (1996).
- ²²D.K. Biegelsen, R.D. Bringans, J.E. Northrup, and L.-E. Swartz, *Phys. Rev. Lett.* **65**, 452 (1990).
- ²³A. Ohtake, J. Nakamura, T. Komura, T. Hanada, T. Yao, H. Kuramochi, and M. Ozeki, *Phys. Rev. B* **64**, 045318 (2001).

This is the author's peer reviewed, accepted manuscript. However, the online version of record will be different from this version once it has been copyedited and typeset.
PLEASE CITE THIS ARTICLE AS DOI: 10.1116/6.0003957

- ²⁴T. Hayakawa, M. Morishita, and S. Chen, Appl. Phys. Lett. **59**, 3321 (1991).
- ²⁵A. Taguchi, K. Shiraishi, and T. Ito, Phys. Rev. **60**, 11509 (1999).
- ²⁶T. Ito, K. Shiraishi, H. Kageshima, and Y. Suzuki, Jpn. J. Appl. Phys. **37**, L488 (1998).
- ²⁷L.Ö. Olsson, L. Ilver, J. Kanski, P.O. Nilsson, C.B.M. Andersson, U.O. Karlsson, M.C. Håkansson, Phys. Rev. B **53**, 4734 (1996).
- ²⁸S.Y. Tong, G. Xu, and W.N. Mei, Phys. Rev. Lett. **52** 1693 (1984).
- ²⁹A. Taguchi, K. Shiraishi, and T. Ito, Phys. Rev. **61**, 12670 (2000).
- ³⁰M.R. Fahy, K. Sato, and B.A. Joyce, Appl. Phys. Lett. **64**, 190 (1994).
- ³¹K.D. Vallejo, T.A. Garrett, K.E. Sautter, K. Saythvy, B. Liang, and P.J. Simmonds, J. Vac. Sci. Technol. B **37**, 061810 (2018).